QUANTUM MECHANICS

2015 © The Authors, some rights reserved; exclusive licensee American Association for the Advancement of Science. Distributed under a Creative Commons Attribution NonCommercial License 4.0 (CC BY-NC).
10.1126/sciadv.1400222

Critical flow and dissipation in a quasi–one-dimensional superfluid

Pierre-François Duc,[1] Michel Savard,[1] Matei Petrescu,[1] Bernd Rosenow,[2] Adrian Del Maestro,[3] Guillaume Gervais[1,4]*

In one of the most celebrated examples of the theory of universal critical phenomena, the phase transition to the superfluid state of ^{4}He belongs to the same three-dimensional (3D) O(2) universality class as the onset of ferromagnetism in a lattice of classical spins with *XY* symmetry. Below the transition, the superfluid density ρ_s and superfluid velocity v_s increase as a power law of temperature described by a universal critical exponent that is constrained to be identical by scale invariance. As the dimensionality is reduced toward 1D, it is expected that enhanced thermal and quantum fluctuations preclude long-range order, thereby inhibiting superfluidity. We have measured the flow rate of liquid helium and deduced its superfluid velocity in a capillary flow experiment occurring in single 30-nm-long nanopores with radii ranging down from 20 to 3 nm. As the pore size is reduced toward the 1D limit, we observe the following: (i) a suppression of the pressure dependence of the superfluid velocity; (ii) a temperature dependence of v_s that surprisingly can be well-fitted by a power law with a single exponent over a broad range of temperatures; and (iii) decreasing critical velocities as a function of decreasing radius for channel sizes below $R \simeq 20$ nm, in stark contrast with what is observed in micrometer-sized channels. We interpret these deviations from bulk behavior as signaling the crossover to a quasi-1D state, whereby the size of a critical topological defect is cut off by the channel radius.

INTRODUCTION

Motivation

Helium is the only known element in nature that becomes a superfluid, with its small mass and weak polarizability cooperating to prevent solidification at atmospheric pressure as the temperature approaches absolute zero. For ^{4}He, the ability to flow without viscosity below the λ-transition temperature, T_λ, is a paradigmatic manifestation of emergent phenomena and macroscopic quantum coherence, driven by both interactions and bosonic quantum statistics. Its superflow with velocity $v_s = (\hbar/m)\nabla\Phi$ is caused by a quantum-mechanical phase gradient of the wave function and *a priori* should only be limited by the Landau criterion of superfluidity. The existence of the roton minimum in the excitation spectrum sets this value to be $v_L \simeq 60$ m/s. However, years of experiments (*1*) have shown that superfluid ^{4}He exhibits a critical velocity that is well below v_L. Although there is consensus that superfluid helium dissipates energy by creating vortex rings, the exact microscopic dynamics that govern the nucleation of topological defects remain an open problem in condensed matter physics.

At first glance, it would appear that this problem would only be exacerbated as the number of spatial dimensions decreases because enhanced thermal and quantum fluctuations should push $T_\lambda \to 0$. However, in the one-dimensional (1D) limit, the universal quantum hydrodynamics of Tomonaga-Luttinger liquid theory (*2*–*4*) should apply, providing a host of theoretical predictions including the simultaneous algebraic spatial decay of both density-density and superfluid correlation functions. Although there is a body of evidence of this exotic behavior in low-dimensional electronic systems (*5*–*8*) and ultracold low-density gases (*9*), the analogous behavior has yet to be confirmed experimentally in a highly correlated bosonic liquid. Here, the physics of superflow should be qualitatively altered, with the superfluid density ρ_s acquiring system size and frequency dependence (*10*). Furthermore, neutral mass flow transport properties should be strongly modified in 1D, with the superfluid velocity v_s exhibiting non-universal power law dependence on temperature and pressure. This crossover toward 1D is manifest in the main findings of our work: (i) a suppression of the pressure dependence of v_s for $R \simeq 3$ nm indicative of enhanced dissipation via phase slips, (ii) a temperature dependence for v_s that can be described by a power law with a single exponent over a broad range of temperatures, and (iii) decreasing critical velocities as the radius decreases for channel sizes below $R \simeq 20$ nm, behavior strongly deviant from what is observed in micrometer-sized channels.

Length scales

In this work, the mass flow rate of superfluid helium is measured in a capillary experiment through channels with radii as small as $R \simeq 3$ nm and length $L = 30$ nm. To determine the effective dimensionality of this geometry, it is imperative to perform a comparative analysis of all possible relevant length scales. Unlike superconductors and superfluid ^{3}He, which undergo BCS pairing, ^{4}He has a very small coherence length on the angstrom scale: $\xi_4(T) \simeq \xi_0(1 - T/T_\lambda)^{-\nu}$, with $\xi_0 \simeq 3.45$ Å and $\nu \approx 2/3$, making it technically difficult to fabricate a transverse confinement dimension with $R \ll \xi_4$ approaching the truly 1D limit, as, for example, $\xi_4 \sim 0.5$ to 1.5 nm in the temperature range considered here. For $T = 0.5$ to 2 K, R can also be compared to the thermal de Broglie wavelength, $\Lambda(T) = \sqrt{2\pi\hbar^2/mk_BT} \sim 1$ nm and a thermal length $L_T = \hbar c_1/k_BT \sim 1$ nm, where $c_1 \simeq 235$ m/s is the first sound velocity of ^{4}He. Another estimate of the effective dimensionality can be obtained by considering helium atoms confined inside a long cylinder of radius R with hard walls. In analogy with electrons confined in quantum wires, we compute the energy needed to populate excited

[1]Department of Physics, McGill University, Montreal, Quebec H3A 2T8, Canada. [2]Institut für Theoretische Physik, Universität Leipzig, D-04103 Leipzig, Germany. [3]Department of Physics, University of Vermont, Burlington, VT 05405, USA. [4]Canadian Institute for Advanced Research, Toronto, Ontario M5G 1Z8, Canada.
*Corresponding author. E-mail: gervais@physics.mcgill.ca

single-particle transverse modes, and find that to fill the lowest excited transverse angular momentum state for a single helium atom, a temperature $T \sim \Delta_\perp/k_B \simeq 3.5/R^2$ nm^2 · K ~ 0.4 K for R = 3 nm is needed. These estimates, which mostly neglect interaction effects, would place our flow experiments in a mesoscopic regime, with confinement length and energy scales on the order of the intrinsic ones in the problem. However, recent ab initio simulations of ^{4}He confined inside nanopores (*11*, *12*) have demonstrated that classical adsorption behavior leads to an effective phase separation between a quasi-1D superfluid core of reduced radius and concentric shells of quasi-solid helium near the pore walls. This effect, which is likely also present in our channels, would tend to provide additional confinement, allowing us to investigate a nontrivial dimensional crossover.

Previous investigations of helium confined at the nanometer scale have focused on porous media such as in Vycor (*13*) and more recently in the zeolites and other mesoporous media. These studies have shown a possible new thermodynamic phase of ^{4}He stabilized at low temperature (*14*) as well as a nuclear magnetic resonance (NMR) signature of a 1D crossover for ^{3}He (*15*). Although these advances are certainly considerable in the search for a strongly interacting 1D neutral quantum liquid, our approach differs much in spirit from those cited above. In our experiment, the helium atoms are confined inside a *single, nearly cylindrical* pore, rather than in an extremely large number of them necessary to gain a signal for a macroscopic probe. This lone pore, or channel, is tailor-made from a pristine Si_3N_4 membrane that can be fabricated with radii ranging from R ~ 1 to 100 nm. The main advantage of our approach is that there is no ensemble averaging over pore distributions and/or potential defects of the sample. Its main drawback, however, is that traditional bulk measurement techniques, such as specific heat or NMR, most likely cannot be performed in a single nanopore containing only ~10^4 to 10^5 helium atoms. Taken as a whole, these two approaches are complementary to one another and similar in spirit to "bottom-up versus top-down" or "single-molecule versus ensemble-averaged" studies in other fields, such as nanoelectronics or molecular biology.

RESULTS

Mass flow measurements

Above T_λ, in the normal phase of helium, the flow through the nanopore is viscously dissipative and expected to follow the model developed for a short pipe by Langhaar (*16*). In this phase, we conducted pressure sweeps at constant temperature while monitoring the mass flow rate Q_m, as shown in Fig. 1 (A and B). In the absence of a chemical potential difference, the mass flow rate should go to zero. However, we observe a spurious signal as $\Delta P \rightarrow 0$ arising from evaporation at the walls of the channel. To determine this offset, the data were fitted with the flow equation for short pipe,

$$Q_n = \frac{8\pi\eta L}{\tilde{\alpha}}\left(\sqrt{1+\frac{\tilde{\alpha}\rho R^4}{32\eta^2 L^2}\Delta P}-1\right) \quad (1)$$

where η is the viscosity, ρ is the density, and $\tilde{\alpha}$ is a coefficient to take into account the acceleration of the fluid at the pipe end (see the Supplementary Materials). In Fig. 1 (A and B), the solid line is a fit to the data with a radius of R = 7.81 ± 0.15 nm and 3.14 ± 0.11 nm. The mass flow was then measured as a function of temperature across the superfluid phase transition T_λ at several pressures for both pores. These data are displayed in Fig. 1 (C and D), with the offset previously discussed subtracted. Previous work in Vycor (*13*) has found the superfluid transition to be suppressed to 1.95 K; however, the superfluid transition in our channels is observed at the temperature corresponding to the bulk value, 2.17 K. This is not surprising because we measure the total conductance of the nanopore channel and of the source reservoir in series, so the onset of superfluidity in the bulk is first observed at T_λ. Considering only data below T_λ, we can extract the superfluid velocities using the two-fluid model, where we assume $Q_{tot} = Q_n + Q_s = (\rho_n v_n + \rho_s v_s)\pi R^2$ with the n and s subscripts denoting the normal and superfluid components of the fluid, respectively. Subtracting Q_n from the total mass flow using Eq. 1 yields the superfluid portion of the flow with a velocity $v_s = Q_s/\pi R^2 \rho_s$. The superfluid density is taken from the bulk, as justified by previous work in Vycor (with a similar network pore size), albeit with a lower transition temperature (*13*). The extracted superfluid velocities are shown in Fig. 2A for the lower-pressure data sets, where linear response is expected to be a better approximation and where the data sets were taken over a large range of temperatures. An inspection by eye readily shows that the superfluid velocities are smaller in the $R \simeq 3$ nm pore at similar pressures and temperatures. Such suppression of the flow velocity as the radius is decreased is in stark contrast with the bulk behavior and shows that dissipation is increasing as the radius of the pore approaches a few nanometers.

Near the bulk superfluid transition, it is well established that the superfluid density follows a universal power law form $\rho_s \sim (1 - T/T_\lambda)^\nu$,

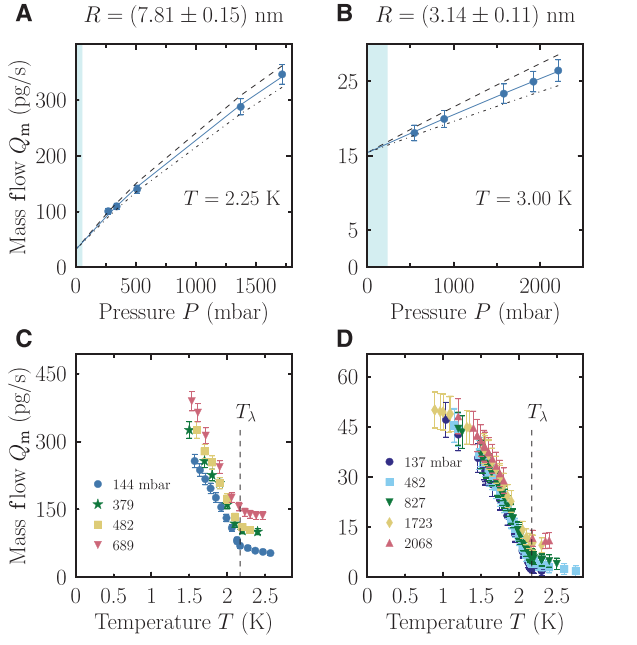

Fig. 1. Flow measurements raw data. (**A** and **B**) Mass flow measurements as a function of pressure for (A) a 7.81-nm and (B) a 3.14-nm pore radius in the normal state. The blue line is a fit of the data using Eq. 1, and the dashed and dash-dotted lines are 1 SD from the mean value for the radius, with all other parameters kept constant. The finite intercept value at zero pressure is a spurious signal (see the text). (**C** and **D**) Temperature dependence of the mass flow at several pressures. The dashed line shows the known superfluid transition temperature (T_λ) at saturated vapor pressure.

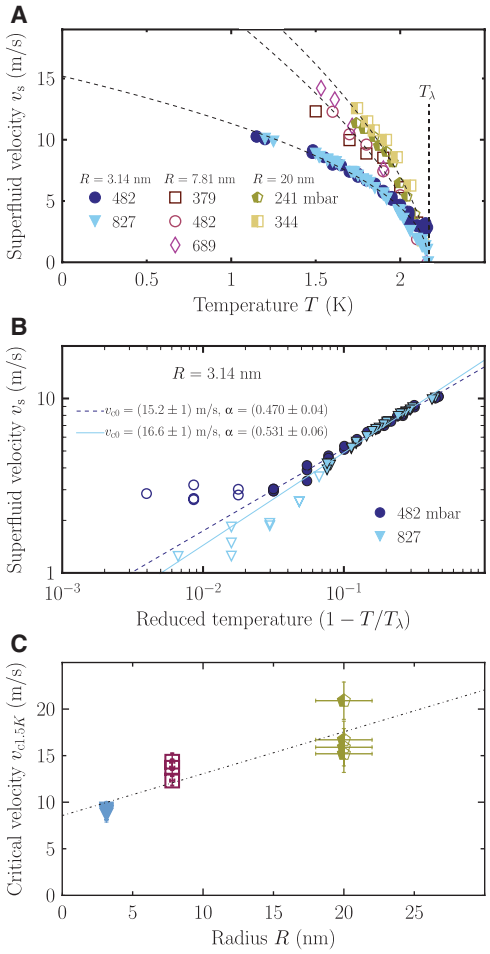

Fig. 2. Superfluid velocities. (**A**) The superfluid velocities are shown at several pressures below 1 bar for three different nanopore radii. The filled symbols refer to the 3.14-nm pore, the open symbols to the 7.81-nm pore, and the half-filled symbols to a 20-nm pore from a previous study (*21*). The dashed lines are fits using the power law $v_s(T) = v_{c0}\left(1 - \frac{T}{T_\lambda}\right)^\alpha$ (see the text). (**B**) Log-log plot of the superfluid velocity versus the reduced temperature for the 3.14-nm pore data. The data used for the power law fit are highlighted with filled symbols. The fits are shown by a dashed line (482 mbar) and a solid line (827 mbar). (**C**) Critical velocity in the nanopores extracted at 1.5 K temperature (plotted at several pressures less than 1 bar) to compare with previous work in much larger channels (see the Supplementary Materials). The superfluid velocities are assumed to be reaching the critical velocity. The dotted line is a blind linear fit shown here only as a guide to the eye.

where ν is a correlation length critical exponent found experimentally to be close to 2/3. Considering a slowly varying quantum-mechanical wave function with a phase Φ, the kinetic energy of the superfluid is given by $\rho_s v_s^2/2 = \rho_s\left(\hbar^2/2m^2\right)|\nabla\Phi|^2$. From scale invariance, we expect that near T_λ, the mean square of the superfluid velocity should scale with the correlation length $\xi_4(T)$ as $\overline{v_s^2} \sim 1/\xi_4(T)^2 \sim (1 - T/T_\lambda)^{2\nu}$. This result is, strictly speaking, valid only at temperatures very close to T_λ, $(1 - T/T_\lambda) \lesssim 0.1$. From this hyperscaling analysis, there is no reason to expect power law behavior in the superfluid velocity over a wide range in temperature away from T_λ. However, in the data shown in Fig. 2A, a power law $v_s(T) = v_{c0}\,(1 - T/T_\lambda)^\alpha$, where v_{c0} is the superfluid critical velocity at $T = 0$ K, was used to fit all the data. A log-log plot of v_s versus the reduced temperature is shown in Fig. 2B for the 3.14-nm pore. For this radius, where very little pressure dependence on the flow is observed, the power law yields an exponent 0.53 ± 0.04 and 0.47 ± 0.06 for the low-pressure (482 mbar) and higher-pressure (827 mbar) data set, respectively, and their critical velocities at zero temperature are v_{c0} = 15.2 ± 1 m/s and 16.6 ± 1 m/s. In contrast, the larger pore (7.81 nm) displays a significantly distinct exponent 0.66 ± 0.05 and zero-temperature critical velocity v_{c0} = 30.1 ± 2.4 m/s. Although not a proof, given the limited range in temperature explored, the appearance of a smaller non-universal exponent as the dimensionality is reduced is consistent with expectations from quantum hydrodynamics in 1D where increased fluctuations should prohibit long-range order.

Dissipation mechanisms

Other important features of the flow data not previously observed are (i) the extremely weak pressure dependence below T_λ for the smaller pore, and (ii) an overall decrease in critical velocity as the channel size is reduced, in contrast to the behavior $v_c \sim \frac{\hbar}{mR}\ln\left(\frac{R}{a_0}\right)$, with a_0 the size of the vortex core, predicted by Feynman and found in larger channels (see the Supplementary Materials). The former is a hallmark of the macroscopic phase coherence that exists in a superfluid phase, in sharp contrast with the Euler prediction of a classical inviscid fluid, $v_s = \sqrt{2\Delta P/\rho_s}$. Using the Gibbs-Duhem relation to convert a pressure to chemical potential difference, energy conservation dictates that there must exist a dissipation mechanism in the channel with a rate Γ such that $h\Gamma = \frac{m\Delta P}{\rho_s} - \frac{1}{2}mv_s^2$. From our data, it is clear that the dissipation rate must be flow (pressure)–dependent. The question of how energy is dissipated in superfluids has a long history, beginning with the proposal of Anderson (*17*) that, in analogy with the Josephson effect in superconductors, a steady-state non-entropic flow may be achieved at a critical velocity v_c via a mechanism that unwinds the phase of the order parameter in quanta of 2π. Such "phase slips," occurring at rate Γ, correspond to a process whereby the amplitude of the order parameter is instantaneously suppressed to zero at some point along the channel and can be driven by either thermal or quantum fluctuations. Momentum conservation dictates that such events can only occur in the presence of broken translational invariance along the pore (*18*).

Microscopically, dissipation occurs through the creation of quantized vortex rings, the topological defects of superfluid hydrodynamics. In our experiments, the size of critical vortex ring R_c plays a crucial role, and it is determined by the equilibrium condition between the relative frictional force between the normal and superfluid component and the hydrodynamic forces acting on the ring in the presence of flow. Energetically, this manifests as a competition between a positive vortex energy that scales linearly with radius and a negative kinetic core energy scaling like its area. Langer and Fisher (*19*) found $R_c \sim 3$ nm below T_λ, exactly the length scale of the smallest pore considered here. When $R < R_c$, the maximum size of a vortex ring is constrained by the radius of the channel, and thus the energy barrier for their creation is lowered, leading to increased dissipation and an upper bound on v_s set by the Feynman critical velocity. The suppression in the observed critical velocity at T = 1.5 K as a function of decreasing radius shown in Fig. 2C can then be interpreted as a crossover to a regime where flow is dominated by the physics of the channel. As the channel radius continues to decrease further, it is expected that backscattering of helium atoms at low temperature in the guise of

quantum phase slips will increase, resulting in a continued suppression of the critical velocity.

This argument does not address the actual rate, or probability per unit space time that topological defects are created, and experimental estimates of Γ were first made by Trela and Fairbank (*20*), who found Γ ~ 1 Hz for superfluid flow through constrictions with $R \sim 10^{-4}$ m. For the nanoscale pores considered here, we estimate that Γ ~ 3 to 5 GHz, well below the flow rate of 7.5×10^{12} atoms/s measured in our smaller pore, yet approaching the quantum of mass flow $q = m^2/h \sim 10^{10}$ atom/s at 1 bar differential pressure and fluid density taken at saturated vapor pressure.

CONCLUSION

The behavior of superfluid helium flow was studied in capillary channels down to ~3-nm radius. For the smaller pore, the superfluid velocity can be well described by a power law, and it was found to be significantly smaller than in larger channels. This likely signals the crossover to a quasi-1D state whereby increased fluctuations and interaction renormalization are modifying superfluidity. As the channel size is reduced even further, near, or into the subnanometer range, we expect to observe physics characteristic of the truly 1D limit. Here, the algebraic decay of the superfluid order parameter will manifest itself as a reduction of the superfluid density as a function of channel length L and the appearance of non-universal power laws in the mass flow dependence on pressure ($Q_{1D} \sim \Delta P^{\beta}$) and temperature ($Q_{1D} \sim T^{\gamma}$). Additionally, the ratio of the length of the channel to a 1D phase coherence length $\ell_{\Phi} \sim 1/T$ will play an important role in the quantitative theoretical description of our data. Such observations would be markedly different than that seen due to the macroscopic quantum coherence of bulk helium and would signal the experimental discovery of a 1D bosonic quantum liquid.

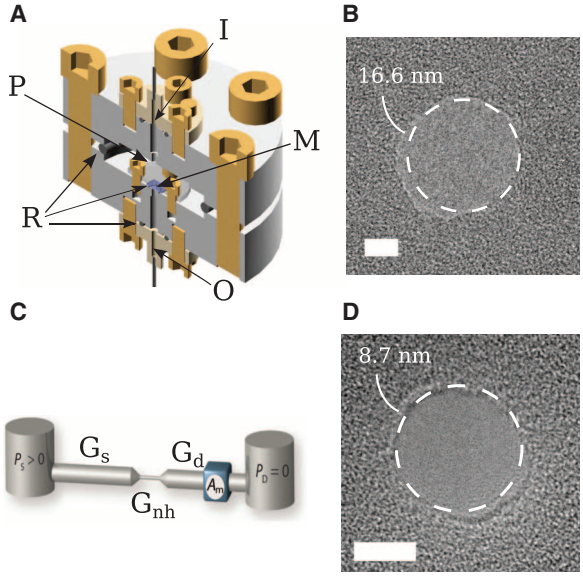

Fig. 3. Design of the capillary flow experiment. (**A**) CAD (computer-aided design) drawing of the coin silver experimental cell. The inlet (I) and outlet (O) reservoir are connected to the top and bottom parts of the cell, and sealed with indium o-rings (R). The SiN membrane (M) is itself sealed to the bottom part of the cell with an indium o-ring and a push-on plate (P). (**B**) Illustration of the flow experiment where the source reservoir is kept at a pressure $P_S > P_D \simeq 0$ and the flow measured by mass spectrometry (A_m) in a series experiment. (**C** and **D**) TEM picture of two nanopores used in this experiment. The bars represent 5 nm in both pictures. The diameter shown here is only an upper bound because the pore undergoes relaxation and its diameter decreases in size after fabrication. In the experiment, the experimental pore radius was determined in situ using both Knudsen effusion in the gas phase and viscous flow measurements in the normal phase of liquid helium.

MATERIALS AND METHODS

The experiment is configured in a similar fashion and follows the same procedure as previously reported in (*21*, *22*). However, the present work is performed in a newly designed experimental cell made out of coin silver and shown in Fig. 3A. The single nanopores were fabricated in the Si_3N_4 membrane using an electron beam from a field effect transmission electron microscope (FE-TEM), with images taken shortly after fabrication shown in Fig. 3 (B and D). Although the single pores have a well-defined diameter, we have observed in previous work that their structure has a tendency to relax at room temperature, with the pore radius decreasing as a function of time (see the Supplementary Materials). To circumvent the uncertainty in the pore dimension, Knudsen effusion measurements in the gas phase of helium were conducted at low temperature (77 K) using the protocol discussed in (*23*). The respective values obtained for each of the pores were determined to be $R^{Kn} = 8.2 \pm 0.5$ nm and 3.10 ± 0.35 nm (see the Supplementary Materials).

In a second step, the experimental cell was cooled down to liquid helium temperature (below 4.5 K). Above T_{λ}, in the normal phase of helium, the flow through the nanopore is viscously dissipative and expected to follow the model developed for a short pipe by Langhaar (*16*). In this phase, we conducted pressure sweeps at constant temperature while monitoring the mass flow rate Q_m, as shown in Fig. 1 (A and B). In the absence of a chemical potential difference, the mass flow rate should go to zero. However, we observe a spurious signal as $\Delta P \rightarrow 0$ arising from evaporation at the walls of the channel. To determine this offset, the data were fitted with the flow equation for short pipe (Eq. 1). In Fig. 1 (A and B), the solid line is a fit to the data with a radius of $R^{He_I} = 7.81 \pm 0.15$ nm and 3.14 ± 0.11 nm. These values are in excellent agreement with those determined independently via Knudsen effusion measurements. It demonstrates *de facto* that our experiment can quantitatively determine the mass flow near the λ-transition in very small channels.

SUPPLEMENTARY MATERIALS

Supplementary material for this article is available at http://advances.sciencemag.org/cgi/content/full/1/4/e1400222/DC1

Text

Fig. S1. Flow measurements.

Fig. S2. Nanopore structural stability.

Fig. S3. Determination of the radius by Knudsen effusion.

Fig. S4. Critical velocities versus channel size.

Reference (*24*)

REFERENCES AND NOTES

1. E. Varoquaux, Critical velocities in superfluids and the nucleation of vortices. *C. R. Phys.* **7**, 1101–1120 (2006).
2. F. D. M. Haldane, "Luttinger liquid theory" of one-dimensional quantum fluids. I. Properties of the Luttinger model and their extension to the general 1D interacting spinless Fermi gas. *J. Phys. C: Solid State Phys.* **14**, 2585 (1981).

3. F. D. M. Haldane, Effective harmonic-fluid approach to low-energy properties of one-dimensional quantum fluids. *Phys. Rev. Lett.* **47**, 1840 (1981).
4. A. Del Maestro, M. Boninsegni, I. Affleck, ^{4}He Luttinger liquid in nanopores. *Phys. Rev. Lett.* **106**, 105303 (2011), and references therein.
5. H. Ishii, H. Kataura, H. Shiozawa, H. Yoshioka, H. Otsubo, Y. Takayama, T. Miyahara, S. Suzuki, Y. Achiba, M. Nakatake, T. Narimura, M. Higashiguchi, K. Shimada, H. Namatame M. Taniguchi, Direct observation of Tomonaga–Luttinger-liquid state in carbon nanotubes at low temperatures. *Nature* **426**, 540–544 (2003).
6. O. M. Auslaender, H. Steinberg, A. Yacoby, Y. Tserkovnyak, B. I. Halperin, K. W. Baldwin, L. N. Pfeiffer, K. W. West, Spin-charge separation and localization in one dimension. *Science* **308**, 88–92 (2005).
7. Y. Jompol, C. J. B. Ford, J. P. Griffiths, I. Farrer, G. A. C. Jones, D. Anderson, D. A. Ritchie, T. W. Silk, A. J. Schofield, Probing spin-charge separation in a Tomonaga-Luttinger liquid. *Science* **325**, 597–601 (2009).
8. D. Laroche, G. Gervais, M. P. Lilly, J. L. Reno, 1D-1D Coulomb drag signature of a Luttinger liquid. *Science* **343**, 631–634 (2014).
9. M. A. Cazalilla, R. Citro, T. Giamarchi, E. Orignac, and M. Rigol, One dimensional bosons: From condensed matter systems to ultracold gases. *Rev. Mod. Phys.* **83**, 1405 (2011).
10. T. Eggel, M. A. Cazalilla, M. Oshikawa, Dynamical theory of superfluidity in one dimension. *Phys. Rev. Lett.* **107**, 275302 (2011).
11. B. Kulchytskyy, G. Gervais, A. Del Maestro, Local superfluidity at the nanoscale. *Phys. Rev. B* **88**, 064512 (2013).
12. L. Pollet, A. B. Kuklov, Topological quantum phases of ^{4}He confined to nanoporous materials. *Phys. Rev. Lett.* **113**, 045301 (2014).
13. G. M. Zassenhaus, J. D. Reppy, Lambda point in the ^{4}He-Vycor system: A test of hyperuniversality. *Phys. Rev. Lett.* **83**, 4800 (1999).
14. R. Toda, M. Hieda, T. Matsushita, N. Wada, J. Taniguchi, H. Ikegami, S. Inagaki, Y. Fukushima, Superfluidity of ^{4}He in one and three dimensions realized in nanopores. *Phys. Rev. Lett.* **99**, 255301 (2007).
15. B. Yager, J. Nyéki, A. Casey, B. P. Cowan, C. P. Lusher, J. Saunders, NMR signature of one-dimensional behavior of ^{3}He in nanopores. *Phys. Rev. Lett.* **111**, 215303 (2013).
16. H. L. Langhaar, Steady flow in the transition length of a straight tube. *J. Appl. Mech.* **9**, A55–A58 (1942).
17. P. W. Anderson, Considerations on the flow of superfluid helium. *Rev. Mod. Phys.* **38**, 298 (1966).
18. S. Khlebnikov, Quasiparticle scattering by quantum phase slips in one-dimensional superfluids. *Phys. Rev. Lett.* **93**, 090403 (2004).
19. J. S. Langer, M. E. Fisher, Intrinsic critical velocity of a superfluid. *Phys. Rev. Lett.* **19**, 560 (1967).
20. W. J. Trela and W. M. Fairbank, Superfluid helium flow through an orifice near critical velocity. *Phys. Rev. Lett.* **19**, 822 (1967).
21. M. Savard, G. Dauphinais, G. Gervais, Hydrodynamics of superfluid helium in a single nanohole. *Phys. Rev. Lett.* **107**, 254501 (2011).
22. A. E. Velasco, C. Yang, Z. S. Siwy, M. E. Toimil-Molares, P. Taborek, Flow and evaporation in single micrometer and nanometer scale pipes. *Appl. Phys. Lett.* **105**, 033101 (2014).
23. M. Savard, C. Tremblay-Darveau, G. Gervais, Flow conductance of a single nanohole. *Phys. Rev. Lett.* **103**, 104502 (2009).
24. M. J. Kim, M. Wanunu, D. C. Bell, A. Meller, Rapid fabrication of uniformly sized nanopores and nanopore arrays for parallel DNA analysis. *Adv. Mater.* **18**, 3149–3153 (2006).

Acknowledgments: We thank I. Affleck for illuminating discussions and comments. We also thank the $(CM)^2$ facility at Polytechnique Montreal for providing access and help with the TEM. **Funding:** This work was funded by Natural Sciences and Engineering Research Council of Canada (NSERC), the Fonds Québécois de la Recherche sur la Nature et les Technologies FRQNT (Québec), and the Canadian Institute for Advanced Research (CIFAR). **Competing interests:** The authors declare that they have no competing interests. **Data and materials availability:** All data, analysis details, and material recipes presented in this work are available upon request to G.G.

Submitted 17 December 2014
Accepted 8 April 2015
Published 15 May 2015
10.1126/sciadv.1400222

Citation: P.-F. Duc, M. Savard, M. Petrescu, B. Rosenow, A. Del Maestro, G. Gervais, Critical flow and dissipation in a quasi–one-dimensional superfluid. *Sci. Adv.* **1**, e1400222 (2015).